ECS Transactions, 53 (1) 9-16 (2013)
10.1149/05301.0009ecst ©The Electrochemical Society

Challenges of Graphene Growth on Silicon Carbide

R. Yakimova*, G. R. Yazdi, T. Iakimov*, J. Eriksson and V. Darakchieva

Department of Physics, Chemistry and Biology, IFM, Linköping University, SE-58183 Linköping, Sweden
* Graphensic AB, Tröskaregatan 15, SE-58333, Linköping, Sweden

One of the main challenges in the fabrication of device quality graphene is the achievement of large area monolayer graphene that is processing compatible. Here, the impact of the substrate properties on the thickness uniformity and electronic characteristics for epitaxial graphene on SiC produced by high temperature sublimation has been evidenced and discussed. Several powerful techniques have been used to collect data, among them large scale ellipsometry mapping has been demonstrated for the first time. The study is covering all three SiC polytype, e.g. 4H-, 6H- and 3C-SiC in order to reveal eventual peculiarities that have to be controlled during graphene growth. The advantage of the cubic polytype is unambiguously demonstrated.

Introduction

Contemporary CMOS technology is stretched to its scaling limits and new materials with superior transport properties are pursued to fuel the increasing demands of high-speed electronics (1). Currently, InGaAs is used as a channel material for InP-based high electron mobility transistors (HEMTs) which represent the fastest field effect transistors (FETs) to date. Projection shows that III-V materials will struggle to obtain the required *fT* = 850 GHz (cut-off frequency – top frequency for current modulation), *fmax* = 1.2 THz (maximum oscillation frequency – top frequency for power modulation). The operation time of a FET is determined by the channel mobility, and the gate current requires a large free-charge carrier density within the channel. High frequencies up to the THz range can be achieved if channel mobility of 10^4-10^5 cm^2/V s and sheet carrier density of 10^{13} cm^{-2} could be realized (2).

Graphene – a single sheet of sp^2-bonded carbon atoms possesses the preferred transport properties surpassing any other known material. When exfoliated (i.e. in free-standing state), graphene has a record room temperature mobility of 200000 cm^2/Vs (3). Note that mechanical exfoliation is unsuitable for large-scale electronic device technology, which would require development of epitaxial graphene with the desired properties. Thermal surface decomposition of SiC substrates currently appears to be the most promising pathway towards wafer-based epitaxy of heterostructures using graphene (3-6). We have shown that by using a high temperature process and Ar gas under highly isothermal conditions, one monolayer graphene over a large area can be reproducibly fabricated (5,6). A recent epitaxial graphene progress report presented *fT* as having reached as high as 300 GHz (7), with the possibility to extend it up to 1THz at a channel length of about 100 nm.

Despite the intense research efforts and remarkable progress, epitaxial graphene with the superior transport properties has not been realized yet. A major concern is the impact of the SiC substrate topology on the uniformity of the electronic properties of epitaxial graphene. In particular, the step bunching that occurs on the SiC surface critically affects the thickness uniformity of epitaxial graphene and the mobility of the free-charge carriers. Substrate defects present additional nucleation sites and lead to differences in growth modes, which may cause thickness and conductivity non-uniformities in graphene.

In this work we discuss the impact of surface status and polytype of the SiC substrate on the quality of the graphene on top. Cubic SiC has the advantage of reduced step bunching which is substantial benefit for acquiring uniform step distribution of a Si-C bilayer size during sublimation. Having the lead of fabricating own 3C-SiC substrates, we present a comparison of the graphene morphology for growth on the hexagonal 6H-, 4H- and cubic 3C-SiC. We confer wrinkles formation and their appearance in epitaxial graphene grown on different surfaces. We use spectroscopic ellipsometry mapping in order to probe the uniformity of the epitaxial graphene thickness on a cm-scale and discuss the effect of substrate polarity on graphene thickness uniformity.

Experimental details

For epitaxial graphene fabrication on SiC we used a reversed sublimation growth process in inductively heated furnace at 2000^{o}C and argon pressure of 1 atmosphere. We have employed SiC substrates of all available polytypes, i.e. hexagonal 4H-SiC (0001) and 6H-SiC (0001), and the cubic 3C-SiC (111). The letter orientation provides the same surface template as for the hexagonal structure. Given by the thermodynamic properties of SiC, this material does not experience liquid phase upon heating under normal conditions. Instead it decomposes by forming Si and C containing species. Si vapor spices have much higher partial pressure compared to that of carbon and these ultimately lead to a graphitization of the SiC substrate. By controlling the growth conditions formation of a monolayer graphene is possible. The growth cell is made of high purity dense graphite and is designed to ensure uniform temperature distribution. The latter along with defect free substrate surface are the main prerequisites for growth of highly uniform monolayer graphene. Furthermore, the heating conditions of a SiC substrate surface to fully reconstruct and form a continuous graphene layer have to consider the variations of the silicon to carbon ratio in the gas phase and particularly close to the substrate surface. At lower temperature the silicon escape is more pronounced at defects and the silicon to carbon ratio is rather high due to the large difference in the Si and C vapor pressures given by the SiC sublimation thermodynamics which results in C deficiency near the surface. The ratio of silicon and carbon containing species is decreased with increasing temperature providing more carbon in the growth cell and allowing more uniform and exact graphene layers, while the issue of homogeneous temperature fields over large area becomes more important. Fig. 1 illustrates the growth furnace and the Si/C ratio in the vapor phase upon SiC heating.

For graphene morphology characterization and the surface potential distribution we used atomic force microscopy (AFM) and scanning Kelvin probe microscopy (SKPM), respectively. Spectroscopic ellipsometry (SE) mapping from 1.25 eV up to 5.45 eV was performed with an M2000 rotating compensator ellipsometer from J. A. Woollam Co. The measurements were realized on a circular area of the sample with a diameter of 0.5 cm and with a micro-spot of 30x30 μm^2. Details about the experimental and modeling procedures can be found in Refs. 8-10.

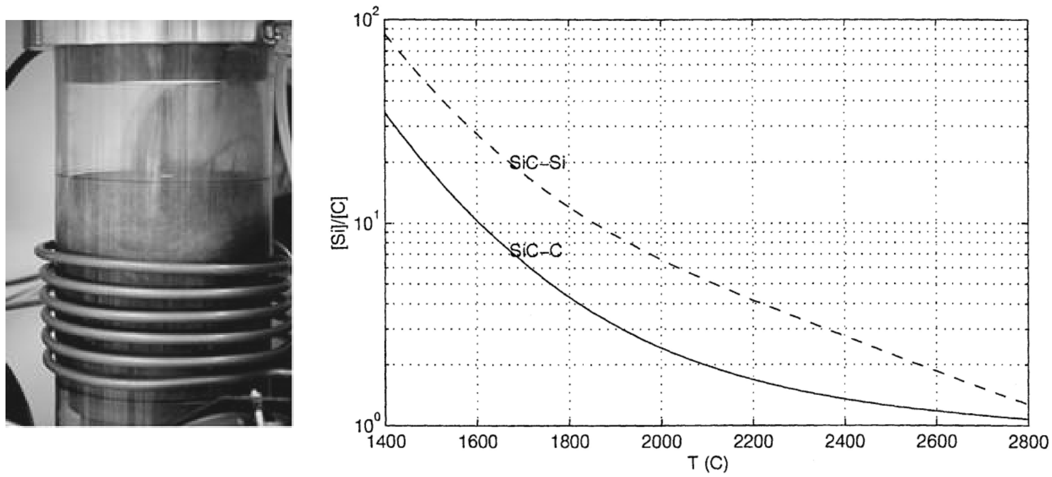

Figure 1. Growth module (left); (right) - Si/C ratio in the vapor phase for two possible equilibrium cases: (i) SiC-Si system and (ii) SiC-C system. Graphene is grown under conditions in case (ii) where complete graphite environment is used.

Impact of surface morphology on graphene characteristiques

By using the above described growth conditions we have fabricated 1ML graphene over a large area, at least 50µm in diameter, with continuous graphene coverage over a two inch wafer. However, variations have been observed in the thickness uniformity and carrier concentration of epitaxial graphene on SiC produced by sublimation for samples grown under identical conditions and on nominally on-axis hexagonal SiC (0001) substrates. We have previously shown that these issues are both related to the morphology of the graphene-SiC surface after sublimation growth (8). The structural and electronic properties of graphene grown on SiC are substrate meditated. A major concern is the natural habit of silicon carbide to cause a step-bunched surface and is a factor to handle for large area graphene growth on silicon carbide wafers. We will further show the impact of the polytype of the SiC substrate on the quality of the graphene on top. Cubic SiC has the advantage of reduced step bunching which is a substantial benefit for acquiring uniform step distribution of a Si-C bilayer size during sublimation.

The thickness uniformity, as shown by SKPM (Fig. 2) and carrier concentration of epitaxial graphene on SiC depend strongly on the terrace width after sublimation growth. There is an optimal terrace with which yields full coverage by only 1ML graphene (Fig. 3) and the Fermi level in that graphene indicates a lower doping compared to graphene formed on not optimal terraces (8). The results in this study indicate that all substrates undergo significant restructuring during the sublimation growth and that the graphene uniformity decreases while the electron doping from the substrate increases with increasing amounts of restructuring (most importantly changes in terrace width). Different samples grown on nominally on-axis hexagonal SiC substrates showed differing restructuring under the same growth conditions, and no correlation was found between the amount of restructuring and the SiC substrate morphology before graphene growth.

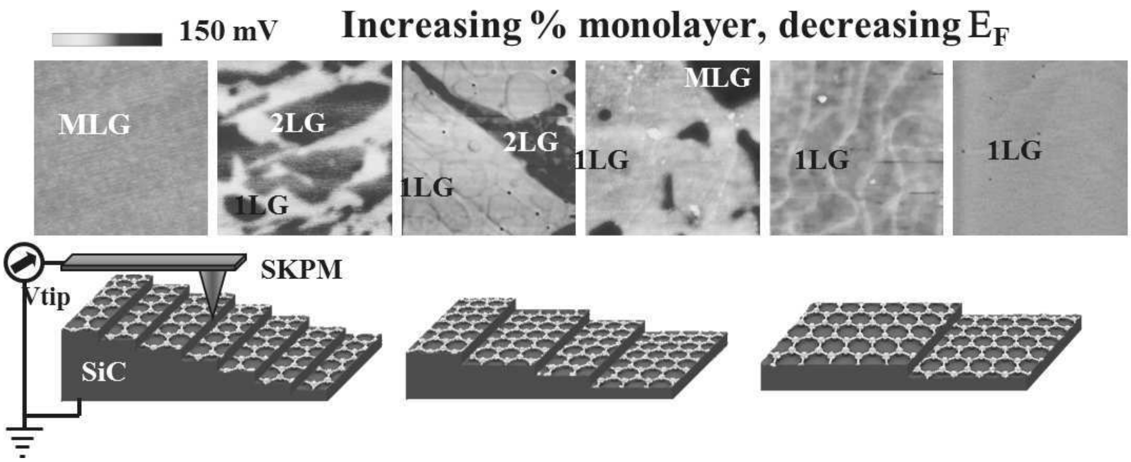

Figure 2. SKPM mapping shows a strong correlation between the graphene thickness uniformity and the surface step morphology

Figure 3 shows how the surface coverage by 1 monolayer graphene changes depending on the terrace with by passing through an optimal value. Fig. 4 illustrates the changes in the graphene thickness uniformity with increasing restructuring; the latter is expressed as a difference in the terrace with before and after substrate thermal decomposition (sublimation).

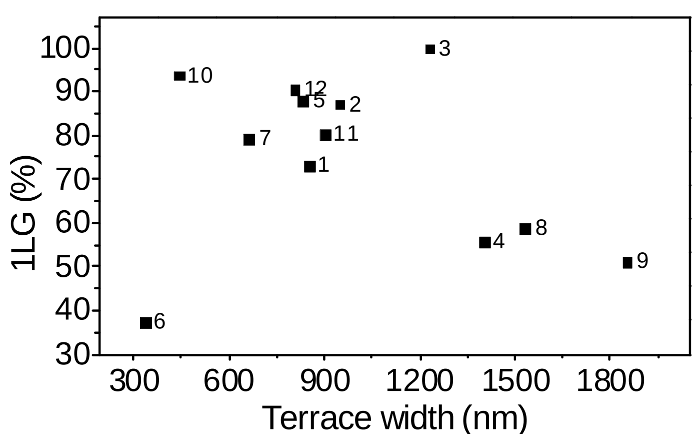

Figure 3. Typical tendency of the graphene monolayer coverage with terrace width for hexagonal SiC substrates. Sample 10 is grown on cubic (3C) SiC substrate.

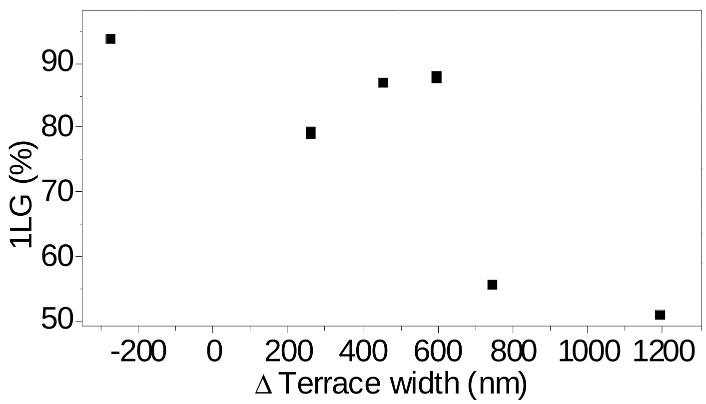

Figure 4. Monolayer graphene coverage vs. surface restructuring.

There may be several considerations on SiC substrate restructuring upon sublimation. A fundamental issue is the so called step bunching which is driven by intrinsic energy minimization, and can be enhanced at the presence of structural defects (11). For the different SiC polytypes, e.g. 4H-, 6H-SiC the stacking sequence along the c-axis is different and the crystal planes have different energies. These result in formation of steps with different heights, typically tending to form one or half a unit cell height, respectively different terraces widths. We have made a statistic over hundreds of steps by using AFM in tapping mode and the results are shown in Fig. 5. One atomic step of SiC is 0.25 nm; the unit cell of 4H SiC is 1nm, and of 6H-SiC it is 1.5 nm. In 3C-SiC all terraces are equivalent and the observed step bunching is only due to defects, typically stacking faults. As seen from the Figure the majority of steps in 4H polytype are grouped at 0.5 and 1 nm, while in 6H-SiC the highest probability of bunching is to 0.5 nm. Concomitantly, 3C-SiC does not experience step bunching besides the small probability grouping dues to defects.

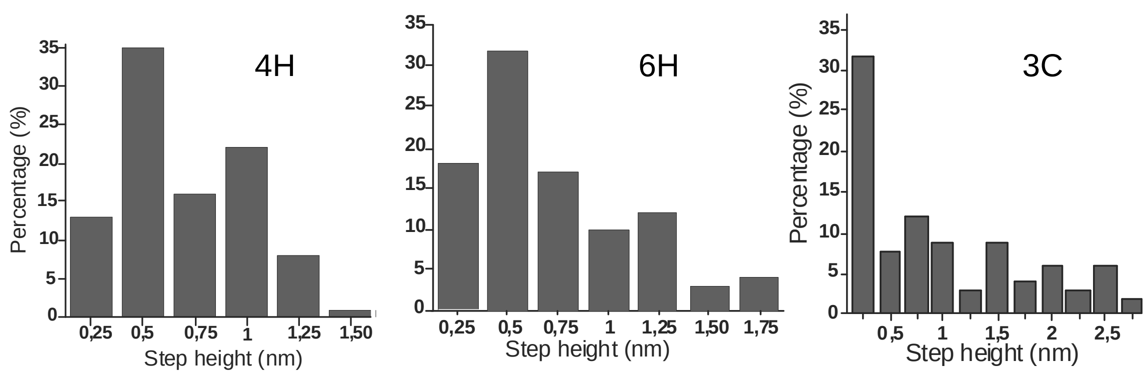

Figure 5. Probability of step height distribution of graphene produced on different substrate polytypes.

Since the step-bunching is significantly smaller in 3C-SiC (111) than in 4H- or 6H-SiC (0001), the cubic polytype is more suitable for obtaining a well-controlled surface morphology after the growth, and is therefore promising for improved control of the electronic properties of the graphene. Graphene grown on 3C-SiC (111) was furthermore found to have lower amount of electron transfer from the substrate as well as generally better uniformity compared to graphene grown on hexagonal SiC.

Surface supported graphene exhibits morphological features often called wrinkles. They are thought to be caused by the thermal compressive strain relaxation. The compressive strain is due to the difference in thermal expansion coefficients between graphene and SiC. Wrinkles are more pronounced on the C-face of SiC, where typically larger number of ML is grown which suggests that the wrinkle size depends on graphene thickness. Figure 6 shows atomic force microscopy images of graphene grown on Si- and C-face of an on-axis 6H-SiC substrate. We have observed that on the Si-face wrinkle orientation depends on the terrace widths. For large terraces which are typically formed on well oriented (on-axis) substrates the wrinkles have random distribution (Fig. 6) indicating that strain is relaxed in all directions. For graphene grown on intermediate terrace size the wrinkle have predominant orientation perpendicular to the terrace edge. This suggests that the strain relaxation occurs predominantly in the direction perpendicular to the terrace. The density of steps is increased with decreasing the terrace width. The thermal strain induced during cooling down is higher at the step edge than on the terrace due to a stronger bonding between graphene and the substrate. Consequently, greater strain relaxation occurs at the edges resulting in wrinkles that are mostly oriented in direction perpendicular to the terrace. Indeed, the wrinkles in graphene grown on substrate with even smaller step widths are only oriented in direction perpendicular to the terrace edge with no component along the parallel direction. We have examined wrinkles with Kelvin probe but no changes of the surface potential have been observed. Also processing Hall bars on graphene containing wrinkles does not show any particular difference from using graphene without wrinkles. This subject however has not been fully explored and needs further attention.

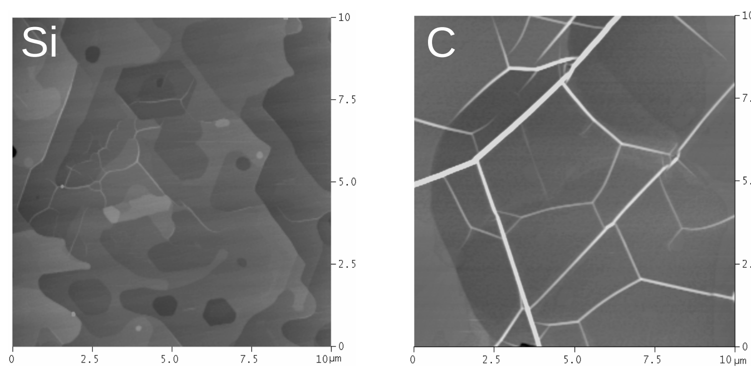

Figure 6. AFM images of wrinkle appearance on the Si and C-face of an on-axis SiC substrate.

Micro-ellipsometry mapping

Figure 7 displays ellipsometry thickness maps of epitaxial graphene grown on the Si-face and C-face of 3C-SiC substrates. The map for the Si-face reveals large homogeneous areas ~2x2 mm^2 with 1 monolayer graphene. Low-energy electron microscopy (LEEM) and Raman scattering spectroscopy confirmed the formation of large-area 1ML graphene in excellent agreement with the ellipsometry mapping. One can also see in Fig. 7 few areas with a size of several hundred micrometers, where the carbon piled up on the surface of the substrate and formed islands of multilayer graphene. On the other hand, for the C-face the graphene thickness varies mostly between 1 to 3 MLs and the formation of thick graphite-like islands is suppressed (Fig.7-right). However, the size of the areas with homogeneous graphene thickness is much smaller in comparison with the Si-face case and only a few domains are 1ML thick. This was also confirmed by LEEM imaging that revealed domains from 0 to 4 MLs with a size down to several micrometers. The analysis of the ellipsometry data further reveals that for the Si-face, the substrate beneath the thick areas is rougher while 1ML graphene grows on relatively smooth surface. A comparison with the substrate morphology indicates that the rougher areas may be associated with surface depressions caused by twin boundaries. It is well known that defects in the SiC substrate serve as preferential centers for enhanced Si sublimation. Thus a higher growth rate of graphene could be expected around these defects, which may explain the formation of the graphite-like islands. On the other hand for the C-face the ellipsometry analysis shows small uncorrelated nucleation sites that have high graphene coverage within the interface layer. We associate these sites with the small pit defects on the C-face that represent 6H-SiC inclusions. Furthermore, we determine the maps of the free-charge carrier scattering time for both polarities. Our results indicate that higher mobility (larger scattering time) can be achieved in the homogeneous areas of 1 ML epitaxial graphene, while the thicker graphite islands show that the carrier mobility drastically decreases. The latter can be related to grain boundary scattering and/or scattering between the different graphene sheets.

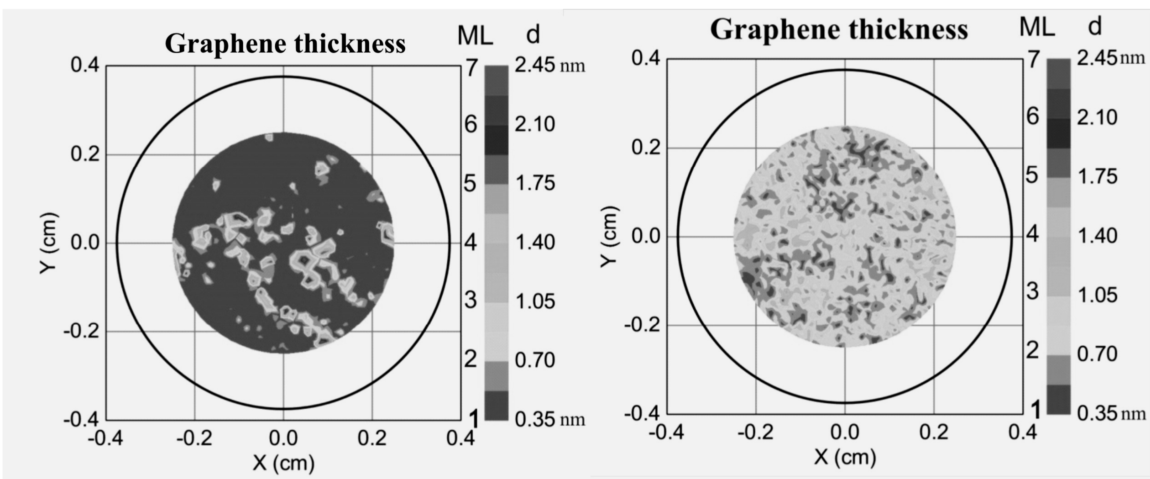

Figure 7. Micro-ellipsometry maps of the thickness of epitaxial graphene grown on Si-face of 3C-SiC (left panel) and C-face of 3C-SiC (right panel).

Conclusion

Thickness uniformity of epitaxial graphene on SiC is impacted by the surface morphology of the substrate and is still an issue. In order to achieve the necessary control care should be taken about the initial substrate surface as well the probability of step formation. There exists a range of optimal terrace width which should be kept in order to maintain formation of 1ML graphene and to avoid increasing of carrier concentration.

The development of micro ellipsometry mapping has allowed probing the thickness uniformity and related parameters on a cm scale. It has been shown that 3C-SiC is a promising substrate for growth of high quality graphene. Differences between Si-face and C-face graphene are revealed. These are related both to the graphene formation mechanism and the substrate morphology.

The availability of large area monolayer graphene produced by our method has allowed demonstration measurements of quantum Hall effect with a high precision surpassing that for exfoliated graphene and being similar to the accuracy achieved in the established semiconductor resistance standards. These results are exceptionally promising for new findings in the metrology (12).

Acknowledgments

We acknowledge support from the Swedish Research Council (VR) under grants No.2010-3848 and No.2011-4447, the Swedish Governmental Agency for Innovation Systems (VINNOVA) under the VINNMER international qualification program, grant No.2011-03486 and the EU project Concept-Graphene.

References

1. H. Iwai, Microelectron. Eng. **86**, 1520 (2009).
2. K. Kodama and M. Kuzuhara, *IEICE Electron. Express* **5**, 1074 (2008)
3. Y.-M. Lin, C. Dimitrakopoulos, K.A. Jenkins et al., *Science* **327**, 662 (2010).
4. C. Berger, Z. Song, X. Li, et al., *J. Phys. Chem. B* **108**, 19912 (2004).
5. C. Virojanadara, M. Syvajarvi**,** R. Yakimova, et al, *Phys. Rev. B* **78**, 245403 (2008).
6. R. Yakimova, C. Virojanadara, D. Gogova, M. Syväjärvi, D. Siche, K. Larsson, L. I. Johansson, Mater. Sci. Forum Vols. **645-648**, 2010, p. 565-568
7. L. Liao et al., Nano Lett. **10**, 39520 (2010).
8. J. Eriksson, R. Pearce, T. Iakimov, C. Virojanadara, D. Gogova, M. Andersson, M. Syväjärvi, A. Lloyd Spetz, and R. Yakimova, Appl. Phys. Lett. **100** (2012) 24160.
9. A. Boosalis, T. Hofmann, V. Darakchieva, R. Yakimova and M. Schubert, Appl. Phys. Lett. **101**, 011912 (2012).
10. A. Boosalis, T. Hofmann, V. Darakchieva, R. Yakimova, T. Tiwald, M. Schubert, and D. Sekora, Mat.Res. Soc. Symp. Proc. **1407**, aa20-43 (2012).
11. G.Reza Yazdi, R. Vasiliauskas, T. Iakimov, A. Zakharov, M. Syväjärvi, R. Yakimova, Carbon (2013) in press.
12. Al. Tzalenchuk, S. Lara-Avila, Al. Kalaboukhov, S. Paolillo, M. Syva¨ja¨rvi, R. Yakimova, O. Kazakova, T. J. B. M. Janssen, V. Fal'ko and S. Kubatkin, Nature Nanotechnology **5.** 186 (2010)